Archaeological Prospection
Archaeol. Prospect. **10**, 163–173 (2003)
Published online 6 August 2003 in Wiley InterScience (www.interscience.wiley.com). DOI: 10.1002/arp.212

Mapping the Ancient Port at the Archaeological Site of Itanos (Greece) Using Shallow Seismic Methods

A. VAFIDIS[1]*, M. MANAKOU[1], G. KRITIKAKIS[1], D. VOGANATSIS[1], A. SARRIS[2] AND Th. KALPAXIS[2]

[1] *Applied Geophysics Laboratory, Mineral Resources Engineering, Technical University of Crete, Chania 73100, Greece*
[2] *Laboratory of Geophysical-Satellite Remote Sensing and Archaeo-Environment, Institute of Mediterranean Studies, Foundation of Research and Technology (F.O.R.T.H.), Rethymno, 74100 Greece*

ABSTRACT A shallow seismic survey was carried out at the archaeological site of Itanos, Crete to locate and map the ancient port. The target layer in the area surveyed consists of Permian–Triassic phyllites covered by alluvial deposits. Seismic refraction and reflection experiments were carried out along eight profiles with a total length 580 m.

The seismic refraction data depict two refractors. Shear-wave velocities indicate that the first refractor, at depths ranging from 1 to 2 m, corresponds to the water table. The second one corresponds to the top of phyllites. The stacked section from the seismic reflection survey shows two major reflectors, attributed to the top and bottom of the eroded phyllites. A three-dimensional image of the basement relief indicated the potential shape and extent of Itanos port.

This result is further supported by anthropogenic anomalies on the resistivity maps and sections observed at locations where the depth to the top of the basement is small. The integration of the seismic data, aerial imagery and archaeological findings indicated that the ancient port, now covered by recent deposits, was surrounded by the sea, the two acropolis to the north, a well to the east and a hill to the south.

Key words: ancient port; seismic refraction; seismic reflection; shear waves

Introduction

The application of seismic methods in archaeological prospection is limited, mainly owing to difficulties associated with the very shallow depth of archaeological targets (Vafidis *et al*., 1995). Seismic, ground-penetrating radar and electromagnetic surveys were conducted by Utecht (1988) and Utecht *et al*. (1993) at a tumulus in Turkey in order to map the stratigraphy of the construction and to locate the monument under the artificial cover. A seismic refraction technique with circular receiver geometry was utilized for the detection of tombs buried in Macedonian tumuli in northern Greece (Tsokas *et al*., 1995). Karastathis and Papamarinopoulos (1997) detected King Xerxes' Canal by the use of reflection and refraction methods. Recently, Washbourne *et al*. (1998) used a direct-arrival transmission imaging technique to detect and delineate underground voids that could possibly house buried treasure.

* Correspondence to: A. Vafidis, Applied Geophysics Laboratory, Mineral Resources Engineering, Technical University of Crete, Chania 73100, Greece. E-mail: vafidis@mred.tuc.gr

Received 25 February 2002
Accepted 2 January 2003

Seismic reflection applications with investigation depths of about 3–6 m (Birkelo *et al*., 1987; Miller *et al*., 1989) encounter difficulties related with the separation of the signal from noise. For shallow reflectors the amplitude of the reflections is often smaller than that of coherent noise (Karastathis and Papamarinopoulos, 1997).

Several geophysical surveys have been reported in archaeological prospecting that combine conventional and high-resolution geophysical methods (Vaughan, 1986; Pipan *et al*., 1996; Vafidis *et al*., in press). Also, aerial photography and satellite imaging are integrated with ground-based geophysical data for archaeological prospecting using geographical Information systems (e.g. Cox, 1992; Donoghue *et al*., 1992; Sarris *et al*., 1998).

In September 1997, a seismic survey was conducted at the archaeological site of Itanos, located in northeastern Crete, Greece (Figure 1). The scope of the seismic survey was to image the subsurface and to map the port of Itanos. Eight refraction profiles were carried out with a total length 580 m and a 70-m-long reflection line.

In this paper, historical remarks about the site and the refraction results are presented. The acquisition, processing and interpretation of the seismic reflection data are described. Additionally, the results from the seismic survey are compared with those from electrical survey.

The archaeological site of Itanos

Itanos, an ancient port in eastern Crete, is located 10 km north of Palaikastro, Lasithi prefecture (Figure 1) close to the, unique in Europe, Vai Palm Forest. The sea to the east, a mountain to the south and the provincial road to the west and north surround the archaeological site. Its area is 16 000 m^2. Archaeological excavations cover only 1% of the archaeological site. There are two hills

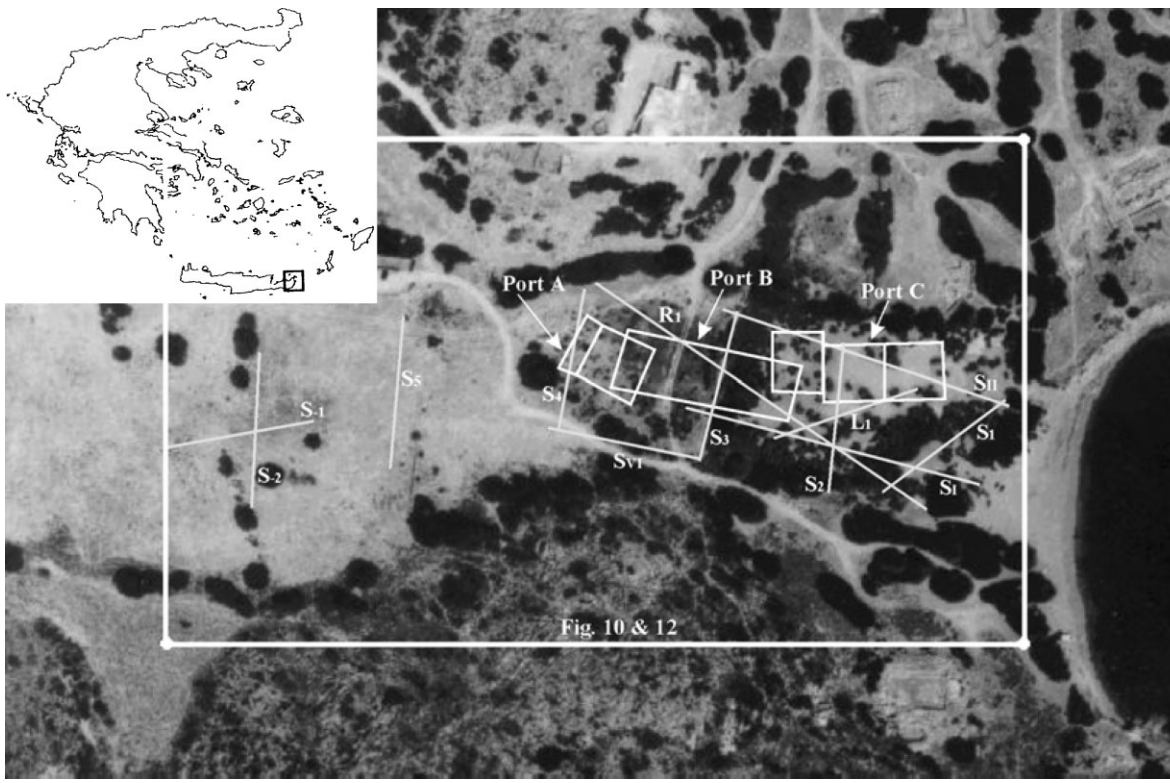

Figure 1. Aerial photograph of Itanos archaeological site showing the surveyed grids and lines. The large frame 'Fig. 10 and 12' refers to the images of Plates 1 and 3. 'Port A', 'Port B' and 'Port C' denote the grids that were scanned using the resistivity method, and 'R1' denotes the electrical tomography line. The symbols S and L indicate the seismic lines.

where the two acropolis of the ancient city were located. Most of the relics of the buildings of the ancient city have been located in the region between the acropolis.

According to an establishment plan common in the Archaic Cretan cities, the houses and the market (agora) are located on the foothills of the two acropolis, whereas the religious monuments are located on the acropolis. A church from the Hellenistic period was found on the western acropolis. South of the acropolis, the region west of the gulf is the potential location of the Itanos port. West of the gulf, there are lowlands crossed by a modern paved road. On the higher hill at the southern border of the lowlands, remnants of fortification walls are still present indicating the establishment of Lagides (Ptolemeoi) army in the fortification (Kalpaxis *et al*., 1995). The inhabited region within the fortification does not exceed 40 ha.

The name of the city according to Stefanos from Byzantium comes from Itanos, the son of Phoenix. Itanos, according to Herodotus the Greek Historian, was one of the most important cities in eastern Crete in the middle of seventh century BC. It is among the first Cretan cities that cut coin (possibly at the beginning of the fourth century BC; Kalpaxis *et al*., 1995; Greco *et al*., 1999).

Demargne, a French archaeologist started excavations at Itanos during the summer of 1899, which led to the detection of the ruins of later Christian period churches and a number of significant Hellenistic and Roman inscriptions (Spyridakis, 1970). In 1950, French archaeologists started a second and more systematic archaeological project. Itanos is marked mainly from three periods: geometric, Roman and late Christian, but periods of original occupation and abandonment are not known. A new archaeological collaborative campaign between the French School of Athens and the Institute of Mediterranean Studies was initiated in 1993. Within the context of archaeological investigations, a geophysical prospecting expedition was also carried out.

The seismic refraction survey

In seismic investigations, seismic waves, created by artificial sources such as a hammer, weight-drop or vibrator, propagate through the earth and are refracted or reflected at interfaces, where the seismic velocity or density changes. Geophones laid on a single line, record the waves returning to the surface after travelling different distances through the ground. By measuring the travel time between the break and the recording of a seismic signal, the seismic velocity in the subsurface and the depth of the interfaces may be inferred. In the seismic refraction method, the above information is deduced from the travel time of the critically refracted seismic waves, which continuously emit seismic energy to the surface and correspond to first arrivals.

The seismic refraction profiles

The purpose of this seismic refraction survey was to map the top of the basement in an effort to define the shape and extent of Itanos port. The target layer in the area surveyed consists of Permian–Triassic phyllites covered by alluvial deposits. Eight P-wave refraction profiles have been selected (Figure 1) with a total length of 580 m and geophone spacing 2 m. The hammer and the seisgun (Betsy) seismic sources, as well as 14 Hz geophones were used in the investiations. Five shots were selected on most seismic lines: one in the middle, two near shots at the edges of the line and two far shots. Typical seismic records for line S_1 are shown in Figure 2.

A limited S-wave refraction experiment has also been conducted along profile L_1 using a shear-wave source and 14 Hz horizontal component geophones. The seismic source consists of a base plate and a large mass placed on top of the plate to provide coupling with the ground. The seismograms obtained by striking the plate on opposite sides, are subtracted in order to remove the P-waves (Lankston, 1990).

For the interpretation of the refraction data, a two-step iteration method was applied (Haeni *et al*., 1987). The algorithm requires an initial depth model, which is obtained from the delay-time method. The algorithm consists of two steps: model-adjustment and ray tracing.

Depth sections were constructed from the modified delay-time inversion method. For line S_I, the top layer exhibits a P-wave velocity of

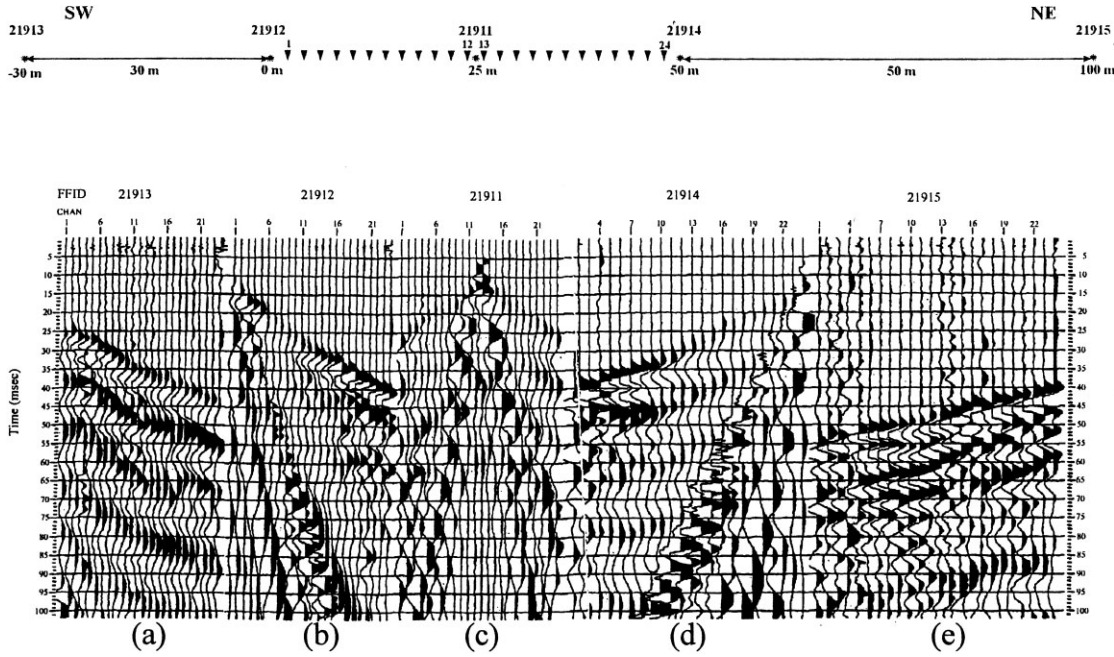

Figure 2. Typical recorded seismic traces for line S_1 corresponding to far offset shots (a and e), near offset shots (b and d) and middle shot (c). The symbol ▼ indicates receiver location and the symbol $^{21912}_{*}$ the shot point and shot number.

448 m s^{-1}. The second layer shows a P-wave velocity of 1741 m s^{-1} and corresponds to water saturated clayey soil (Figure 3a). The deeper layer shows an increased P-wave velocity of 2664 m s^{-1}. This layer is attributed to the phyllites (basement) or to its eroded cover (Table 1). Depth sections were additionally constructed from the P- and S-wave refraction experiments for line L_1 (Figure 4). On these sections, the depths of the refractors correlate well. Shear-wave velocities indicate that the first layer is attributed to unsaturated soils and the second layer to saturated ones (Table 2).

The seismic data for line S_{II} (Figure 3b) were additionally interpreted using the generalized reciprocal method (Palmer, 1981). Velocity analysis indicated lateral velocity variations (Figure 5) for layers 2 and 3. The depths to the second interface from the modified delay-time method (Figure 3b) and the Generalized Reciprocal Method (GRM) (Figure 5) are similar for distances ranging from 30 to 60 m. At these distances the P-wave velocity of the second layer, deduced from GRM (Figure 5), is the same as that obtained from the modified delay-time (Figure 3b). To the east, the modified delay method overestimates this velocity, resulting in increased depths to the second interface. It is also worth mentioning the complexity of the second interface to the west as it is described by both interpretation methods.

Seismic wave propagation simulations were carried out in order to examine the reliability of the velocity and depth models deduced from the seismic refraction survey. Thus, taking into consideration the results of the P-wave refraction of seismic line S_{II}, synthetic seismic data were created using a finite-difference method, which is based on the seismic wave equation (Vafidis *et al.*, 1992). The first breaks on the field and synthetic seismograms were subsequently compared. The relative error exhibits values greater than 10% in two areas for first arrivals corresponding to head waves from the shallow interface (Figure 6). For the deeper interface, namely the top of the basement, this simulation shows that the refraction method calculated acceptable depths and velocities.

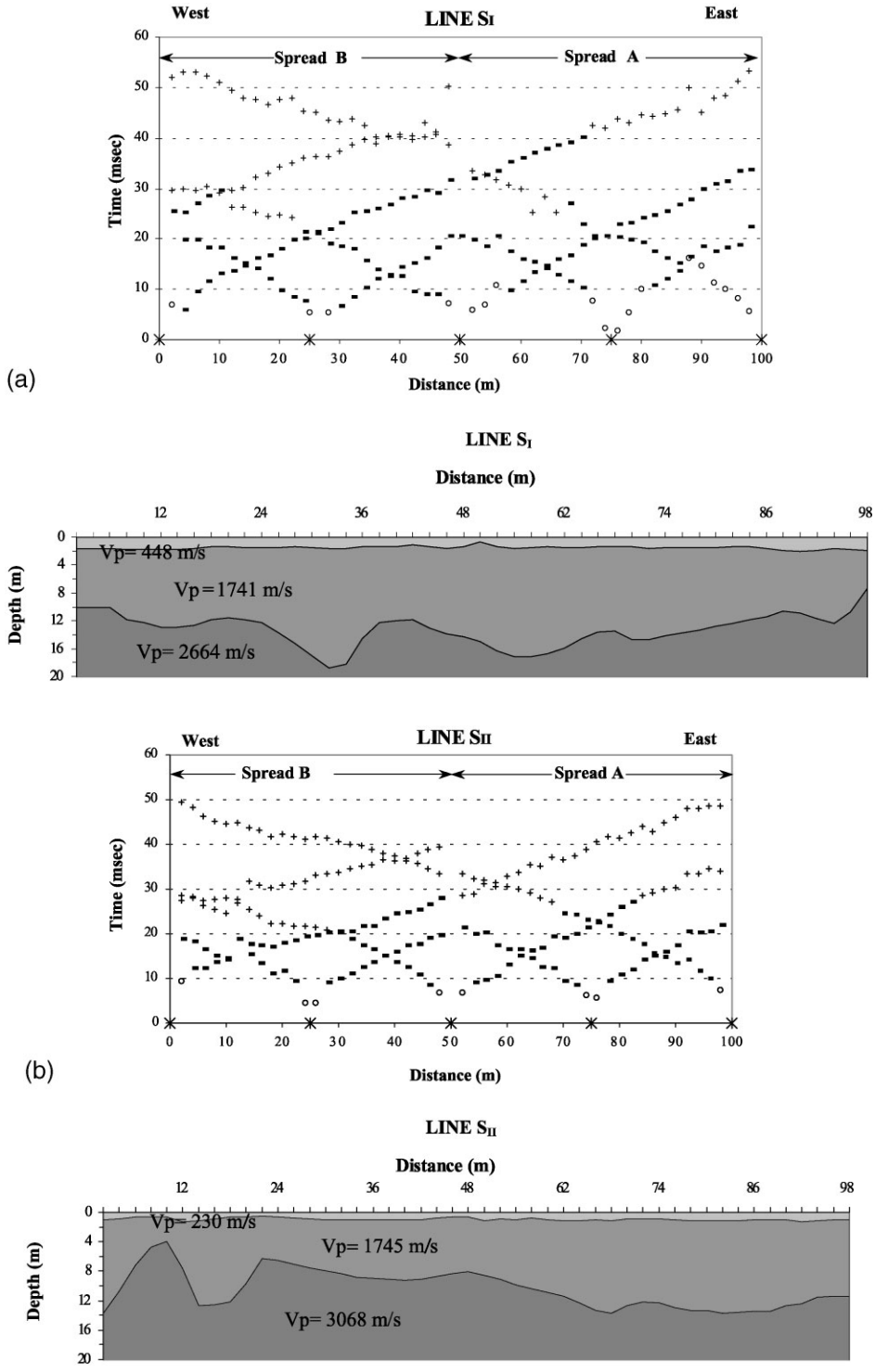

Figure 3. Travel-time curves and depth sections from refraction experiments for lines S_I (a) and S_{II} (b): o, first layer; −, second layer; +, third layer.

Table 1. Velocity and thickness for each layer deduced from seismic refraction data

Survey line	First layer, dry sand: velocity ($m\,s^{-1}$)/ mean thickness (m)	Second layer, wet clayey soil: velocity ($m\,s^{-1}$)/ mean thickness (m)	Third layer, eroded phyllites: velocity ($m\,s^{-1}$)/ mean thickness (m)	Fourth layer, phyllites: velocity ($m\,s^{-1}$)
S_I	448/1.5	1741/8.0	2664	
S_{II}	230/1.0	1745/7.0	3068	
S_1	284/1.0	1537/6.0	2576	
S_2	311/1.0	1452/7.0	2829	
S_3	242/1.0	1845/6.0	3233	
S_4	345/1.0		2541/5.0	3234
S_5	398/2.0		2076/6.0	3615
S_{VI}	278/1.0		2841/15.0	3400
$S_{(-1)}$	770/4.0		1969/5.0	3849
$S_{(-2)}$	924/4.0		1812/5.0	3706
L_1	382/1.2	1728/7.2	2785	

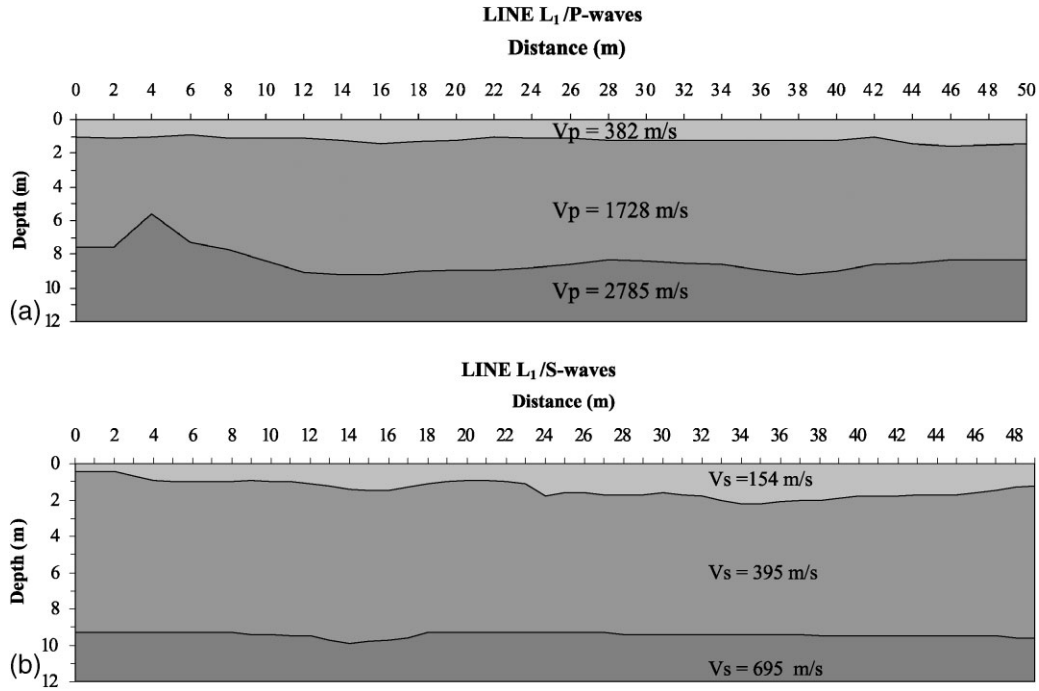

Figure 4. Depth sections from (a) P- and (b) S-wave refraction experiments for line L_1.

Table 2. Distribution of shear-wave velocity, Poisson's ratio and Young modulus

	Layer		
	1	2	3
Rock type	Dry sand	Wet clayey soil	Phyllites
Thickness (m)	1.19 (average)	7.24 (average)	—
Density ($g\,cm^{-3}$)	1.6	2.3	2.65
Vp ($m\,s^{-1}$)	382	1728	2785
Vs ($m\,s^{-1}$)	154	395	695
Poisson's ratio	0.403	0.472	0.467
Young modulus (MPa)	106.5	1056.5	3755.6

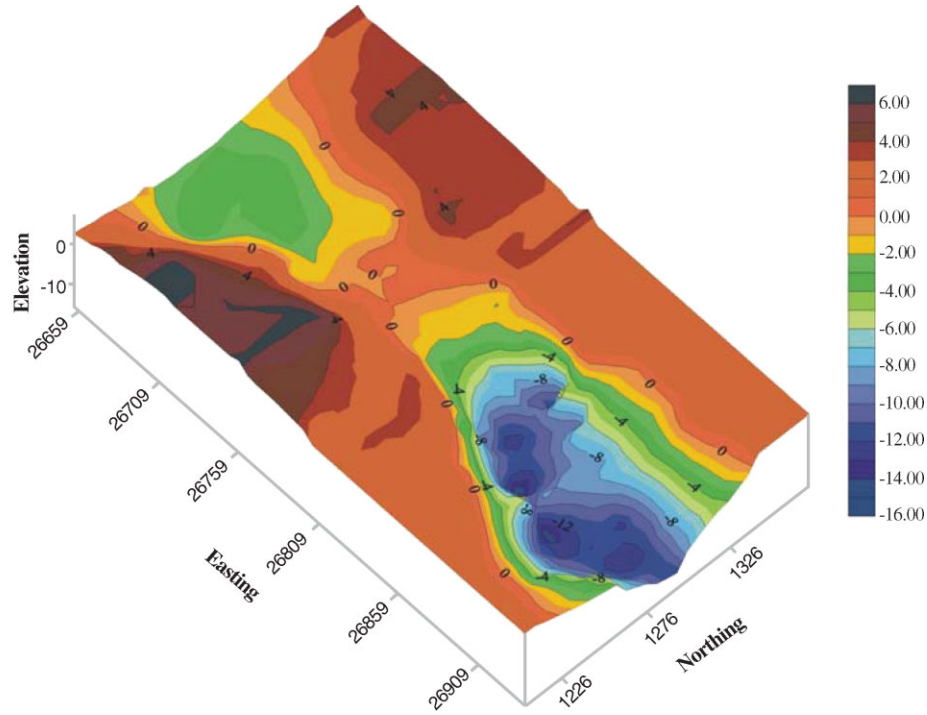

Plate 1. Three-dimensional elevation model of basement indicating Itanos port. The elevations range from 6 m above sea-level to 16-16 m) below sea-level.

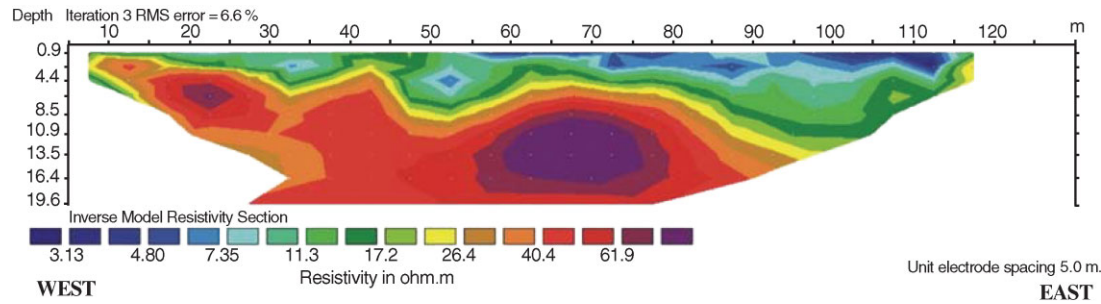

Plate 2(a). Geoelectric sections deduced from electrical tomography for lines B_0.

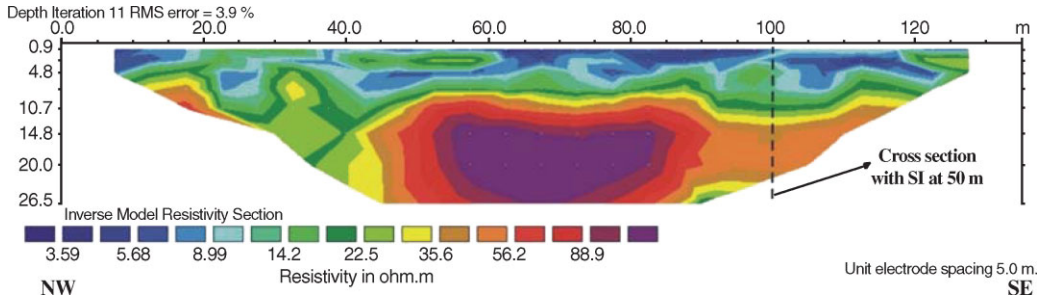

Plate 2(b). R_1. Line B_0 and seismic line S_1 coincide, the former extending longer to the west.

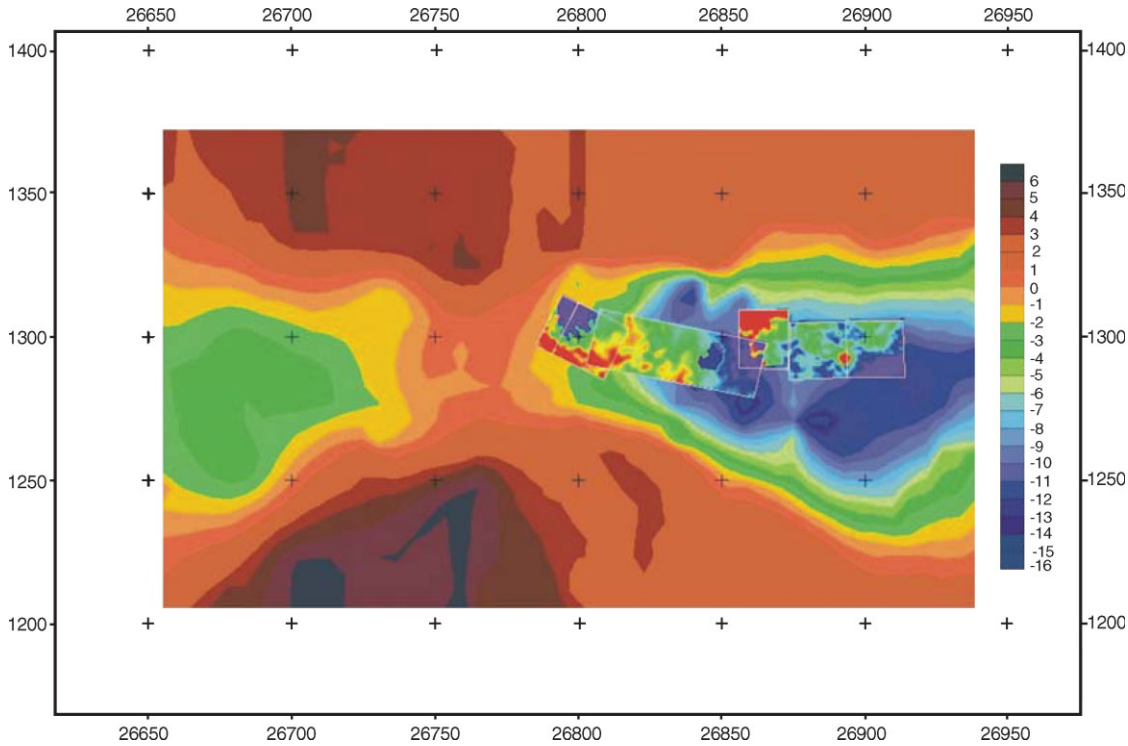

Plate 3. Soil resistance map for grids Port A and Port C and soil conductivity map for grid Port B superimposed on the basement relief map. Red colour on electrical maps corresponds to high resistance.

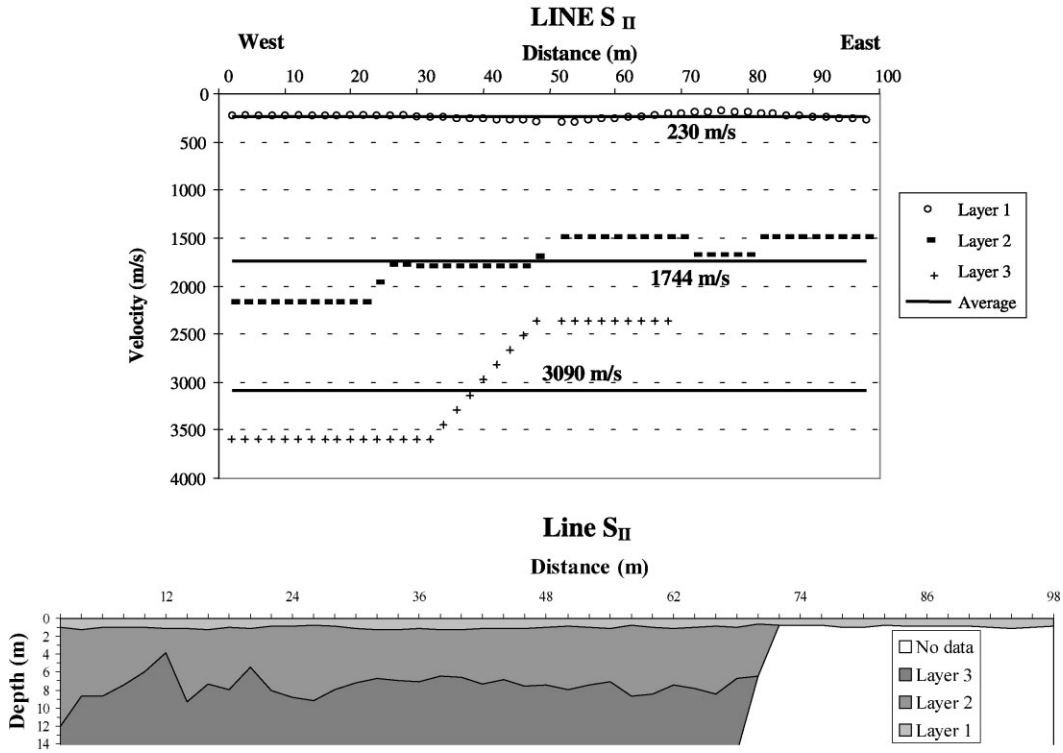

Figure 5. Velocity analysis (up) and depth section (down) computed with the GRM technique for line S_{II}.

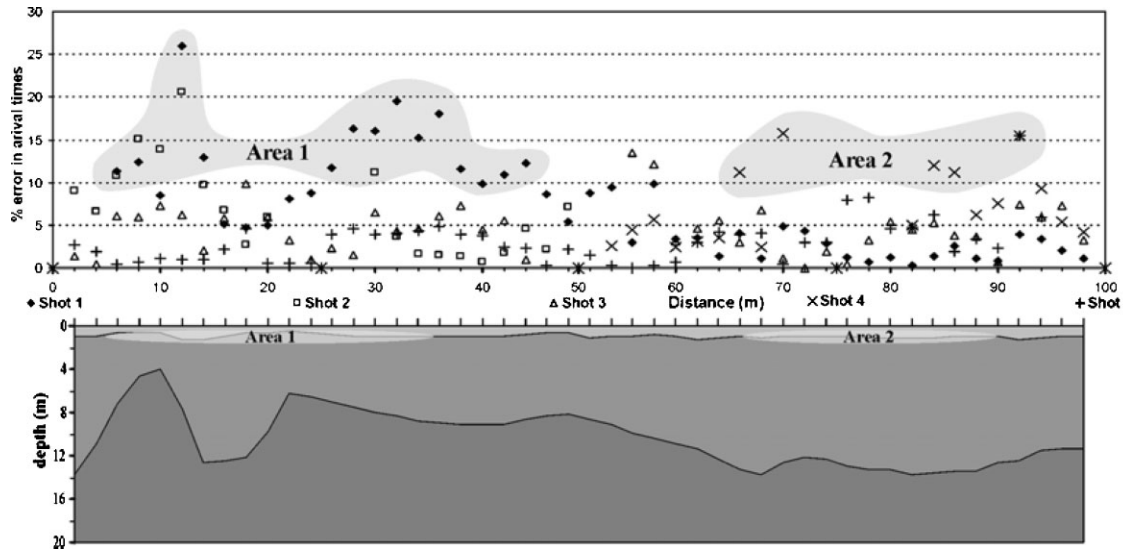

Figure 6. Relative error (up) between the synthetic and field first arrivals for five shots. The synthetic data correspond to the depth section (down) from the refraction experiment for line S_{II}.

The seismic reflection experiment

In the seismic reflection method, the seismic waves are reflected at discontinuities in the ground, i.e. horizons at which the seismic or acoustic impedance changes. The reflected waves are usually received by a string of geophones on the surface. The seismic refraction method requires that the seismic velocity increases with each successively deeper layer. In contrast, the seismic reflection technique involves no prior assumptions about seismic velocity.

A high-resolution reflection survey has been conducted along the line S_I (Figure 1) using the Betsy as the seismic source, with 100 Hz receivers and a 24-channel engineering seismograph (EG&G Geometrics 2401). First, a noise test was performed in order to distinguish signal from noise and to select the optimum source–receiver offsets for the near and far geophones. The geophone spacing was set initially to 2 m and the offset range was 4–98 m. The geophone spacing was then set to 0.5 m and the offset range was 4–100 m.

Taking into consideration the results from the noise test, the sampling interval of the seismic reflection experiment was set to 0.1 ms, resulting in 102 ms record length. The geometry was off-end with a 7 m minimum offset and 0.5 m geophone spacing. The fold of the reflection survey was 600% and the total length of the seismic reflection line was 80 m.

In the reflection survey, the roll-along technique was utilized. The shot interval was set to 1 m, the spacing of Common Depth Points (CDP) was 0.25 m and the number of shots 73. The geometry parameters were selected in order to map the shallow reflectors at depths less than 30–35 m. Figure 7 displays common shot gather records prior (on the right) and after (on the left) filtering with a deconvolution operator. Reflected waves are observed at channels 16–24 between 30 and 35 ms.

Processing of the reflection data, performed with Promax-2D, included transformation from SEG-2 to SEG-Y format, geometry setting of the experiment, trace muting, Automatic Gain Control (AGC), deconvolution, F-K filtering,

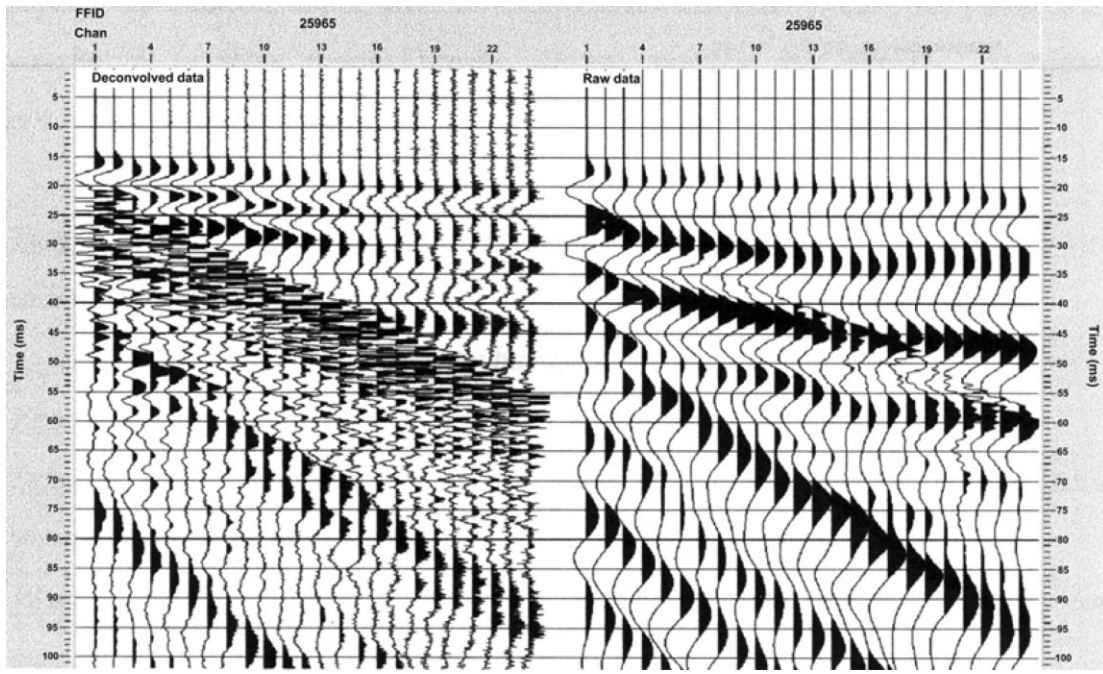

Figure 7. Common shot gather records prior (on the right) and after (on the left) filtering with a deconvolution operator. Reflected waves are observed at channels 16–24 between 30 and 35 ms.

velocity analysis, Normal Moveout (NMO) and stacking. The ground roll and the airwaves were attenuated by frequency-wavenumber (F-K) filtering. This coherent noise was dominant, at times greater than 40 ms. Band-pass filtering partially eliminated the airwaves. The F-K filtering improved the signal-to-noise ratio of the traces by eliminating both ground roll and airwaves.

Two reflectors are present on the stacked section (Figure 8). Reflector 1 (two-way time 21–28 ms and depth 12–19 m) corresponds to the top of the basement. The quality of the reflected waves from a deeper interface (reflector 2) is degraded (two-way time 30–40 ms). Nevertheless, reflectors 1 and 2 exhibit similar relief. Reflector 2 may be attributed to the top of undisturbed phyllites.

The seismic refraction and reflection results for line S_I (Figures 3a and 8) are then compared. The depth to reflector 1 was obtained by converting the two-way travel time to depth using the average velocity of 1400 m s^{-1} for the overlying layers. Reflector 1 and refractor 2 exhibit similar depths (14–19 m) at horizontal distances less than 70 m (Figure 9). Thus, the seismic reflection experiment verifies the refraction survey results, attributing refractor 2 and reflector 1 to the top of the bedrock along the seismic line S_I.

The discrepancy between reflector 1 and refractor 2 at horizontal distances greater than 70 m on seismic line S_I is possibly attributable to

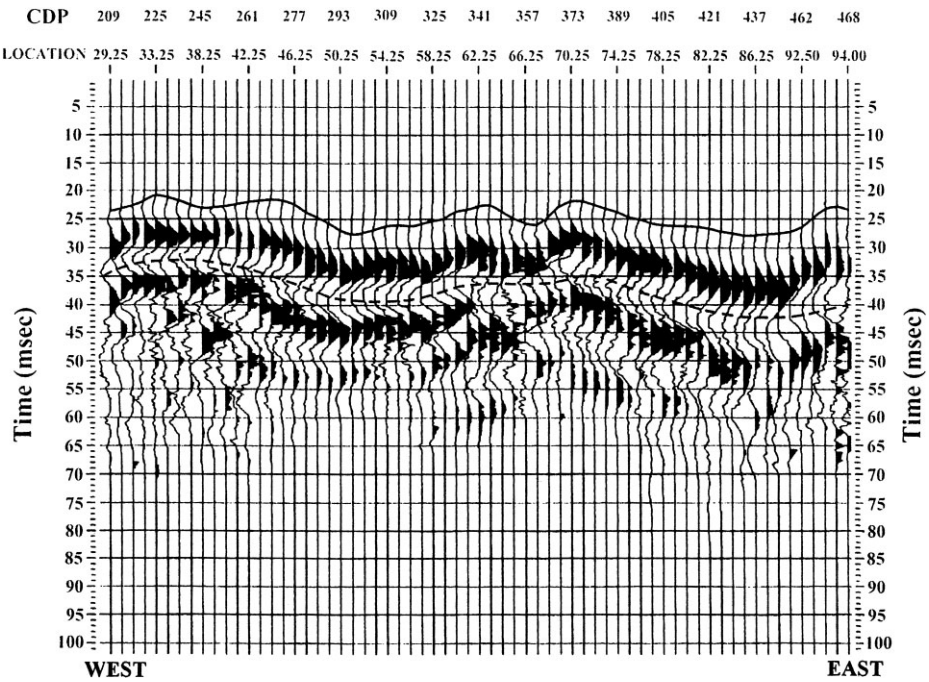

Figure 8. Stacked seismic section along line S_I.

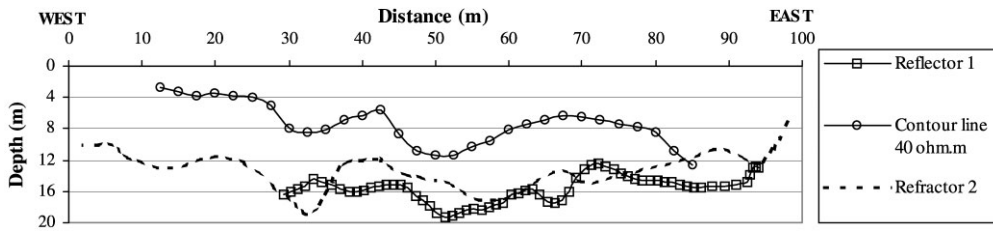

Figure 9. Comparison of seismic and electrical tomography results for line S_I.

lateral velocity variation (Figure 9). According to the velocity analysis performed on the reflection events, the seismic velocity in the overlying recent deposits decreases to the east (less than 20%). This lateral velocity variation relates to depths ranging from 12 to 16 m for reflector 1 at the eastern portion of the seismic line compared with the smaller depths to the refractor 2 (10–14 m).

Comparison of seismic and resistivity results

Seismic, geological and topography data were utilized for the creation of a top-to-the-bedrock image (Plate 1). This image indicates that the ancient port, covered by colluvium, is located south of the acropolis. Its distance to the west from the present seashore is approximately 100 m. It covers an area of approximately 9000 m^2.

Additional remarks can be made from the comparison of the seismic and resistivity results. The resistivity data originate from resistivity sounding and mapping, conductivity mapping and electrical tomography.

A resistivity sounding (Schlumberger array, $AB/2 = 20$ m) along the western portion of seismic line S_{II} indicates three layers. The second is less resistive (11 Ωm) and consists of wet colluvium. This layer exhibits similar thickness (7 m) with the second one (wet colluvium) on the seismic depth section (Figure 5). The third layer (88 Ωm) is attributed to phyllites.

The electrical tomography experiment along the line B_0 was conducted with the dipole–dipole electrode configuration (electrode spacing 5 m). Line B_0 and seismic line S_1 coincide, the former extends longer to the west. The layer with resistivity ranging from 40 to 80 Ωm on the electrical tomography image (Plate 2a) corresponds to wet eroded phyllites. Near the seashore, the image is distorted by the presence of saline water. The top of the basement map, deduced from seismics and the 40-Ωm contour line on the electrical tomography image (Figure 9), exhibit similar features. In particular, both the refractor 2 and the 40-Ωm contour line indicate a pit at horizontal distances 30 to 35 m. Additionally, another pit is observed at horizontal distances 45 to 55 m. The latter feature is also present on the resistivity image (Plate 2b) from the electrical tomography line R_1, which intersects the seismic line S_I at horizontal distance 50 m (100 m on the line R_1).

Soil resistance mapping was carried out on selected grids (Port A, Port B and Port C, Figure 1) utilizing the twin probe array, station spacing of 1 m and electrode spacing of 2 m. Also, quadrature (conductivity) data have been collected with the EM-31 Geonics instrument using the same station spacing. The quadrature data were transformed to resistivity and together with soil resistance data were superimposed on the basement relief map (Plate 3). High resistance anthropogenic anomalies on the geophysical maps correspond to small depths (green colour) to the top of the basement.

Conclusion

This seismic survey indicates that the ancient port was restricted to the rectangular region surrounded by the sea, two acropolis to the north and a hill to the south. The three-dimensional image of the basement relief correlates well with the results from other geophysical surveys such as soil resistance mapping, electromagnetic mapping and electrical tomography. Further geophysical work is required at the zone south and east of the seismic lines S_1 and S_I in order to image better the port entrance. Shear-wave refraction experiments on selected lines were useful for water table verification, being at depths ranging from 1 to 2 m. The top of the basement image obtained by the seismic refraction survey was also verified by the seismic reflection experiment along line S_I. A limited number of shallow boreholes could be useful in verifying the geophysical results.

Acknowledgements

We thank the Department of Mineral Resources Engineering, Technical University of Crete for covering data acquisition cost. We also thank the French School of Archaeology, Athens for providing access to the archaeological site,

Professor G. Tsokas, University of Thessaloniki, Greece, for providing the horizontal component geophones, Professor S. Mertikas for providing GPS data and Mr N. Andronikidis for the seismic wave propagation simulation.

References

Birkelo BA, Steeples DW, Miller RD, Sophocleous M. 1987. Seismic reflection study of a shallow aquifer during a pumping test. *Ground Water* **25**: 703–709.

Cox C. 1992. Satellite imagery, aerial photography and wetland archaeology—an interim report on an application of remote sensing to wetland archaeology: the pilot study in Cumbria, England. *World Archaeology* **24**: 249–267.

Donoghue DNM, Powlesland DJ, Pryor C. 1992. Integration of remotely sensed and ground based geophysical data for archaeological prospecting using a Geographic Information System. *Proceedings of the 18th Annual Conference of the Remote Sensing Society*, Cracknell AP. and Vaughan RA (eds), University of Dundee; 197–207.

Greco E, Kalpaxis Th, Schnapp A, Viviers D, Carando E, De Bonis R, D'Ercole C, Duboeuf P, Francoise J, Garcia Martin C, Grivaud G, Guy M, Licoppe C, Massar N, Sarris A, Schnapp-Gourbeillon A, Theodorescu D, Tsigonaki C, Tsingarida A, Vafidis A, Vitti P, Voza O, Xanthopoulou M. 1999. Travaux menes en collaboration avec l'ecole Francaise d'Athenes en 1998. *Bulletin de Correspondance Hellenique* **123**: 515–530.

Haeni FP, Grantham DG, Ellefsen K. 1987. *Microcomputer-based Version of Sipt. A Program for the Interpretation of Seismic-refraction Data*. Open file report 87-103-A. Harford, CT.

Kalpaxis Th, Schnapp A, Viviers D, Guy M, Licoppe C, Schnapp-Gourbeillon A, Siard H, Theodorescu D, Tsigonaki C, Vafidis A, Xanthopoulou M. 1995. Rapport sur les travaux menes en collaboration avec l'ecole Francaise d'Athenes en 1994. *Bulletin de Correspondance Hellenique* **119**: 713–736.

Karastathis VK, Papamarinopoulos SP. 1997. The detection of King Xerxes' Canal by the use of shallow reflection and refraction seismics—preliminary results. *Geophysical Prospection* **45**: 389–401.

Lankston RW. 1990. High-resolution refraction seismic data acquisition and interpretation. In *Geotechnical and Environmental Geophysics*, Vol. I, Ward SH (ed.). Society of Exploration Geophysicists: Tulsa, Oklahoma; 45–75.

Miller RD, Steeples DW, Brannan M. 1989. Mapping a bedrock surface under dry alluvium with shallow seismic reflections. *Geophysics* **54**: 1528–1534.

Palmer D. 1981. An introduction to the generalized reciprocal method of seismic refraction interpretation. *Geophysics* **46**: 1508–1518.

Pipan M, Finetti I, Ferigo F. 1996. Multi-fold GPR techniques with applications to high-resolution studies: two case histories. *European Journal of Environmental and Engineering Geophysics* **1**: 83–103.

Sarris A, Vafidis A, Mertikas S, Guy M, Kalpaxis Th. 1998. Remote sensing techniques and computer applications for monuments and site assessment of Itanos (E. Crete). Abstracts, *Computer Applications in Archaeology Conference(CAA 98)*, Barcelona.

Spyridakis S. 1970. *Ptolemaic Itanos and Hellenistic Crete*. Zurich.

Tsokas GN, Papazachos CB, Vafidis A, Loukoyiannakis MZ, Variemezis G, Tzimeas K. 1995. The detection of monumental tombs buried in tumuli by seismic refraction. *Geophysics* **60**: 1735–1741.

Utecht T. 1988. Geophysical investigation at the tumulus of Nemrud Dagh, Turkey. In *Engineering Geology of Ancient Works, Monuments and Historical Sites—Preservation and Protection, Proceedings of an International Symposium*, Marinos PG, Koukis GC (eds). Balkema: Rotterdam; 2131–2132.

Utecht T, Lutjen H, Stain B. 1993. Geophysical survey of 1989 at the archaeological site of Nemrud Dagh, Turkey. *Geophysical Exploration of Archaeological Sites*, Vogell A, Tsokas GN (eds). *Theory and Practice of Applied Geophysics* **7**: 249–272.

Vafidis A, Abramovici F, Kanasewich ER. 1992. Elastic wave propagation using fully vectorized high order finite differences. *Geophysics* **57**: 218–232.

Vafidis A, Economou A, Ganiatsos Y, Manakou M, Poulioudis G, Sourlas G, Vrontaki E, Sarris A, Guy M, Kalpaxis A. In press. Integrated geophysical studies in ancient Itanos. *Journal of Archaeological Science*.

Vafidis A, Tsokas GN, Loukoyiannakis MZ, Vasiliadis K, Variemezis G, Papazachos CB. 1995. Feasibility study on the use of seismic methods in detecting monumental tombs buried in tumuli. *Archaeological Prospection* **2**: 119–128.

Vaughan CJ. 1986. Ground penetrating radar surveys used in archaeological investigations. *Geophysics* **51**: 595–604.

Washbourne J, Rector J, Alonso A. 1998. Treasure hunting with direct-arrival transmission imaging. *Leading Edge* **17**: 927–933.

